Dual Mode Electrophoretic Displays with Photoluminescence Electroluminescence, and Three-Dimensional Driving Capabilities

Bo-Ru Yang, Jintao Shi, Xinzao Wu, Guangyou Liu, Yunhe Liu, Junjie He, Kainian Yang, and Longda Li*
State Key Lab. of Optoelectronic Materials and Technologies, Guangdong Province Key Lab. of Display Material and Technology, School of Electronics and Information Technology, Sun Yat-Sen University, Guangzhou 510006, China

***corresponding author: yangboru@mail.sysu.edu.cn**

Abstract

Electrophoretic e-paper has superior optoelectronic properties, such as high ambient contrast, low power, and flexibility. Despite many commercial uses, research continues, exploring on new functions. This paper demonstrates three dual-mode e-papers: with photoluminescence, electroluminescence, and 3D driving. These demonstrations have potential in various applications like anti-counterfeiting, signage, smart windows, etc.

Author Keywords

Electrophoretic e-paper; Multifunctional display; 3D driving; Anti-counterfeiting; signage; Smart window;

1. Introduction

Since the microencapsulated electrophoretic display (EPD) technology was proposed in 1998, which solves the lifetime issues of electrophoretic ink and enables the fabrication of a bistable electronic display through printing methods, EPD technology has become one of the hot topics in display research [1, 2]. EPDs operate based on the movement of charged color particles under an external electric field, reflecting ambient light to perform display images. Compared with transmissive and emissive display technologies, EPDs possess the advantages of low power consumption, wide viewing angle, high ambient contrast, and vision-friendly characteristics [3]. Through the optimization of driving waveform design, the preparation of colored electrophoretic particles, and the introduction of SiPix's microcup encapsulation technology for roll-to-roll inkjet printing electronic paper, full color EPD has been realized, and the production costs have been greatly reduced [4-6]. In line with the era of the Internet of Things and the rapid development of wearable electronics, the current forms of EPDs are no longer limited to flat, rigid devices. Reports of flexible, stretchable, and wearable EPD devices continue to emerge. These wearable electrophoretic electronic paper devices exhibit good stretchability, waterproof and sweat-proof properties, and environmental adaptability, providing important guidance for the structure of wearable displays in future human-computer interactions [7-9].

To investigate more potential applications of EPDs and achieve multifunctional integration and multimodal coexistence in EPDs, our group has explored the integration combining EPD technology with photoluminescence, electroluminescence, and three-dimensional driving, and realized three dual-mode electrophoretic devices as summarized in Figure 1, which demonstrated the integrated functions of these novel multifunctional EPDs beyond their excellent reflective display capabilities.

As shown in Figure 1a, the synthesized novel electrophoretic particles exhibit a white state under visible light and emit green light under ultraviolet (UV) irradiation. The quantum dot materials loaded on white electrophoretic particles leading to different display patterns under visible and UV light illumination. This result confirms the feasibility of using EPDs in dynamic optical anti-counterfeiting and identification [10]. Figure 1b showcases the combination of EPD with alternating current electroluminescence (ACEL) technology [11]. The display layer of the device is composed of microcapsules and ACEL powders doped in polyurethane. The microcapsules and electroluminescent powders operate at different voltages and frequencies, and by adjusting the drive signals, the display can rapidly switch between reflective and emissive states, enabling clear display effects in various lighting environments. Figure 1c shows a 3D driving technology, which forms a 3D spatial electric field with the top common electrode by patterning the bottom electrode [12]. The particles can gather and disperse under the transverse electric field of the bottom electrode to switch between the reflected and transparent states (horizontal mode), and can also move in the longitudinal space to switch between the black and white states (vertical mode), which shows the potential for smart window applications.

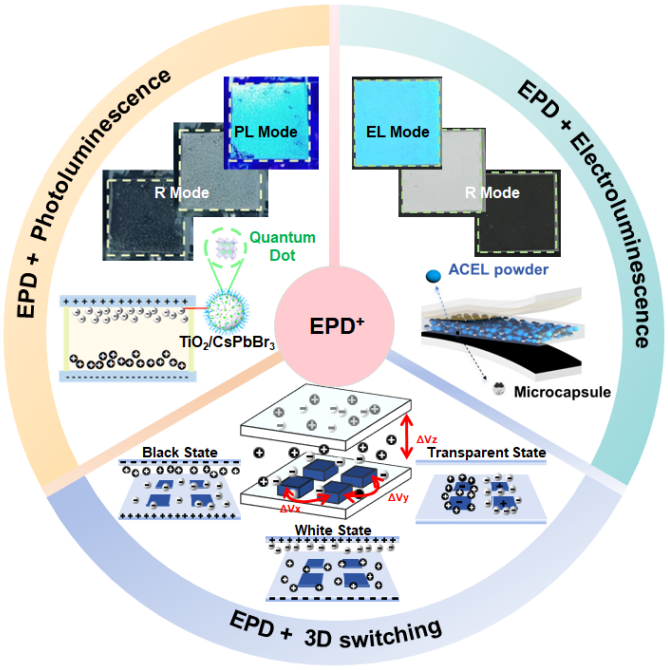

Figure 1. Three types of dual-mode EPD. (a) EPD with doped QD for photoluminescence. (b) EPD with ACEL for electroluminescence. (c) EPD with three-dimensional driving.

2. EPD integrated with photoluminescence

Fluorescent EPDs are suitable for optical anti-counterfeiting because they achieve dynamic patterning, but previously reported fluorescent EPDs suffer from poor display performance, weak fluorescence intensity, and low contrast ratio, which limits their further commercial application [13, 14]. In our study, we have

ISSN 0097-996X/25/5602-1271-$1.00 © 2025

integrated EPD technology with photoluminescence technology. By attaching perovskite quantum dot material $CsPbBr_3$ onto TiO_2 particles and mixing it with $CrCu_2O_4$ black particles, a multifunctional fluorescent anti-counterfeiting EPD device was created, which exhibits a fast response time of 350 ms, a high contrast ratio of 17, and bright green fluorescence.

The synthesis process of the fluorescent electrophoretic white particles is shown in Figure 2 (a). TiO_2 particles have a rich surface of hydroxyl functional groups, which is beneficial for surface modification and grafting of polymers. A comparison of our fluorescent EPD with other reported fluorescent EPDs is depicted in Figure 2 (b). The EPD we prepared has a lower driving voltage of only 15 V and relatively stronger fluorescence intensity. Moreover, our EPD features a response speed of 350 ms and a high contrast ratio of up to 17, enabling this dual-mode fluorescent EPD to achieve good display effects under visible light and excellent anti-counterfeiting applications under UV light.

To further validate the anti-counterfeiting performance of the dual-mode fluorescent EPD, we mixed the synthesized fluorescent electrophoretic white particles with $CrCu_2O_4$ black particles to fabricate an EPD device with the structure shown in Figure 3. The device features transparent ITO glass as the top and bottom electrodes, with the numeral "8" formed by patterned OCA grooves. Five grooves constituting the numeral "2" were filled with ink containing fluorescent electrophoretic particles, while other two grooves were filled with regular electronic ink. Under visible light, the EPD can drive the black and white particles to display the numeral "8" at 30 V. When the fluorescent white particles are driven to the top observation plane, the green fluorescence state of the numeral "2" can be presented by switching to UV light. Conversely, when the EPD is in the black state, the numeral "8" is displayed under ambient light, and no pattern is visible under UV light. Thus, the EPD achieves dynamic anti-counterfeiting and multifunctional display ability.

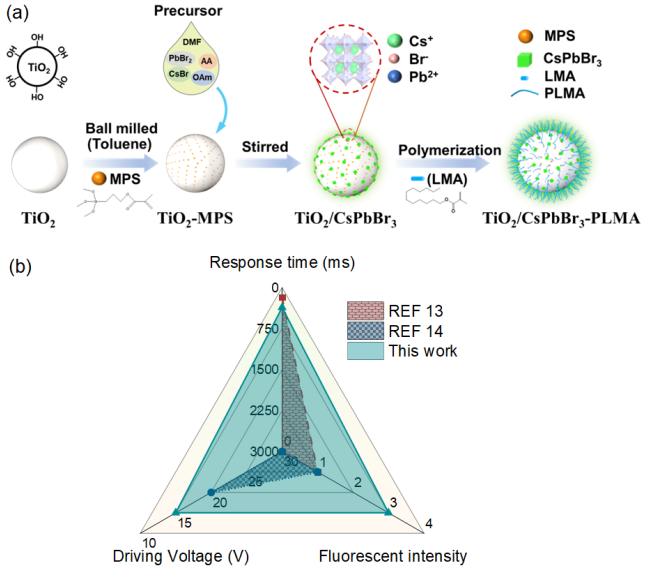

Figure 2. (a) The preparation process of fluorescent electrophoretic particles. (b) The performance comparison of our fluorescent EPD with other reported devices.

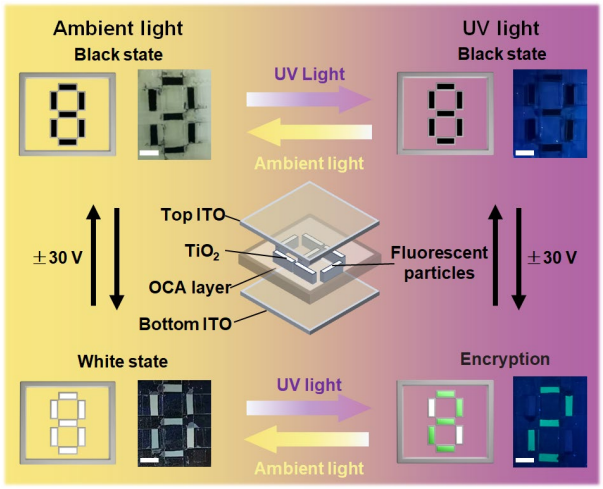

Figure 3. Multifunctional anti-counterfeiting application of the fluorescent EPD. Scale bar：1 cm

3. EPD integrated with electroluminescence

Inevitably, when the ambient light is weak, the visibility and image quality of reflective displays are significantly degraded. The transflective liquid crystal display technology using some pixels for self-luminescent transmissive states and others for reflective states [15]. However, the aperture ratio of transflective displays is low, limiting both brightness and contrast. Additionally, commercial electronic paper signs on the market typically add a front-light module in front of the electronic paper screen to illuminate the display content when ambient light is weak [16]. Nevertheless, this also leads to the complexity of the display module, inability to perform local dimming, and higher energy consumption.

To effectively integrating emissive display with reflective display, our previous research has conducted in-depth investigations into ACEL technology [17, 18], which has significant advantages such as high luminance, low power consumption, and good stability. Similar to electrophoretic electronic paper, ACEL can also be equivalently represented as a series-parallel combination of resistors and capacitors in the circuit model. Therefore, we attempted to introduce ACEL technology into EPDs, achieving an integrated dual-mode electronic paper device with full aperture ratio, a contrast ratio of 5.6, and a brightness of up to 107.5 cd/m² that combines reflective and emissive functions.

The fabrication process of this dual-mode device is shown in Figure 4, which is based on all-solution process. Comparing the performance of our fabricated device with existing dual-mode devices, the results are shown in Table 1. Regarding the response speed for display states, our device has a switching speed of 413 ms /167 ms (white to black/black to white) in reflective mode and 121 ms /2 ms (dark to bright/bright to dark) in emissive mode. To test display stability, the device was driven in cycles for 1000 times, and its stability in both reflective and emissive modes was found to be above 99%, maintaining stable display effects under repeated driving.

Figure 5(a) depicts the mode-switching process of the dual-mode device. By applying positive and negative 24 V voltages, the device, which initially presents a gray state, displays the "SYSU" pattern in black or white. The brightness-Y represents the white light reflectance of the device, characterizing the blackness and whiteness of the device. The operating voltage and frequency for

the emissive mode are relatively higher, our device can maintain the luminance of 27.4 cd/m^2 at a working signal of 150 V, 5 kHz. When a 24 V, 50 Hz shaking waveform is applied, the black and white electrophoretic particles within the microcapsules redisperse uniformly, returning to the initial gray state. Furthermore, through waveform design, our device can also achieve a hybrid mode where both emissive and reflective modes operate simultaneously. As shown in Figure 5(b), by superimposing a positive and negative 24 V DC bias on the working signal, the device can present black and white states with the microcapsules while the ACEL self-luminesces, achieving a light white state (LWS) and a light black state (LBS), thereby making full use of the display area and realizing a richer display effect.

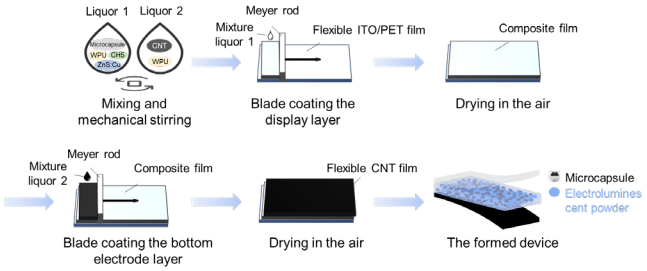

Figure 4. The fabrication process of dual-mode electrophoretic display device integrated with ACEL.

Table 1. The performance comparison with the reported dual-mode display devices.

Ref	Response time		Stability	
	R mode (s)	EL mode (s)	R mode (%)	EL mode (%)
[19]	4 / 3	< 4	50	45
[20]	0.8 / 1.1	1.7 / 2.3	97	94
[21]	4.2 / 6.9	4.9 / 9.7	98.3	99
[22]	0.58 / 0.7	0.57 / 1.8	96	91
This work	0.41 / 0.16	0.12 / 0.002	99.2	100

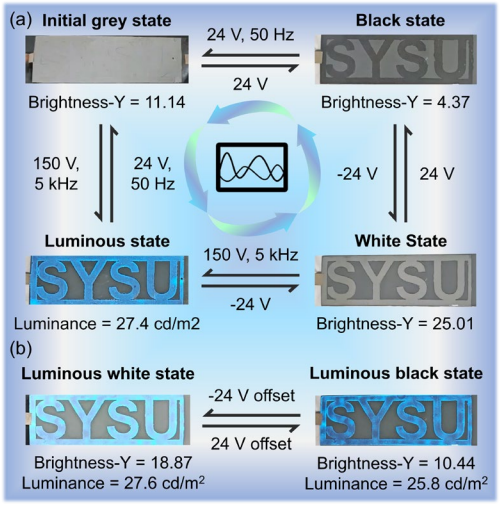

Figure 5. The switching process between different display modes. (a) switching between reflective and emissive modes. (b) switching between luminous white state and luminous black state with bias voltage applied.

4. EPD with three-dimension driving method

In 2014, we proposed the concept of 3D drive for EPD Technology [23]. 3D driving method combines vertical and in-plane driving modes, allowing EPD to switch between reflective and transparent modes. The vertical driving mode can promote the vertical movement of charged particles to achieve different display states, while in-plane driving EPD technology achieves the migration of charged particles within the horizontal plane to achieve transparent state and display states.

The different display states achievable with 3D driving are shown in Figure 6. When black and white particles randomly distributed in the display medium, the device will present a gray state, as shown in Figure 6 (a). When the in-plane driving mode is employed, the electrophoretic particles are attracted to electrodes with opposite charges and stack up on them. Since the pixel electrode (micron scale) can be hidden in the Black Matrix region, the device can be macroscopically transparent without reducing the aperture ratio of the device, as shown in Figure 6 (b). In the vertical drive mode, the vertical electric field drives the particles to move in longitudinal space, achieving a black and white state, as shown in Figures 6(c) and 6(d).

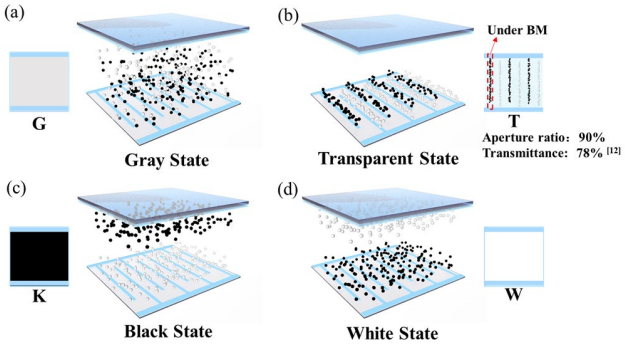

Fig 6. Schematic diagram of different display states in 3D driving EPD. (a) Gray state, (b) Transparent state, (c) Black state, and (d) White state.

To achieve 3D driving, we have designed five different pixel electrode patterns, including square, interdigitated, cross, and double-cross structures, as shown in Figure 7 (a). These electrodes are used to realize the in-plane driven EPD, which verifies the feasibility of the realization of 3D driving [24]. We measured the optical transmittance of the EPD devices in transparent states and the response time of white-to-transparent transition, as depicted in Figure 7 (b). It can be observed that Pattern A achieves the highest transmittance, reaching 67.4%. Pattern C exhibiting the shortest transition time of only 740 ms. It is noteworthy that the transition times can be further optimized through aspects such as driving waveforms and ink formulations.

We designed a 3D driving waveform, as shown in Figure 8. In Step 1, an alternating current voltage is applied to activate particles and enhance mobility. In Step 2, vertical driving is employed. The voltage distribution generates a longitudinal electric field within the device, driving positively charged black particles

to the display side and negatively charged white particles towards the bottom. Subsequently, by reversing the electrode voltages, the electrophoretic particles move to the opposite side, presenting a white state. In Step 4, a horizontal electric field is formed, causing the charged particles to stack on electrodes with opposite charges.

The 3D driving mode EPD technology enables a transition between reflective and transparent modes, which presents substantial potential for application across diverse sectors, including automotive, eyewear, timepieces, and smart window systems.

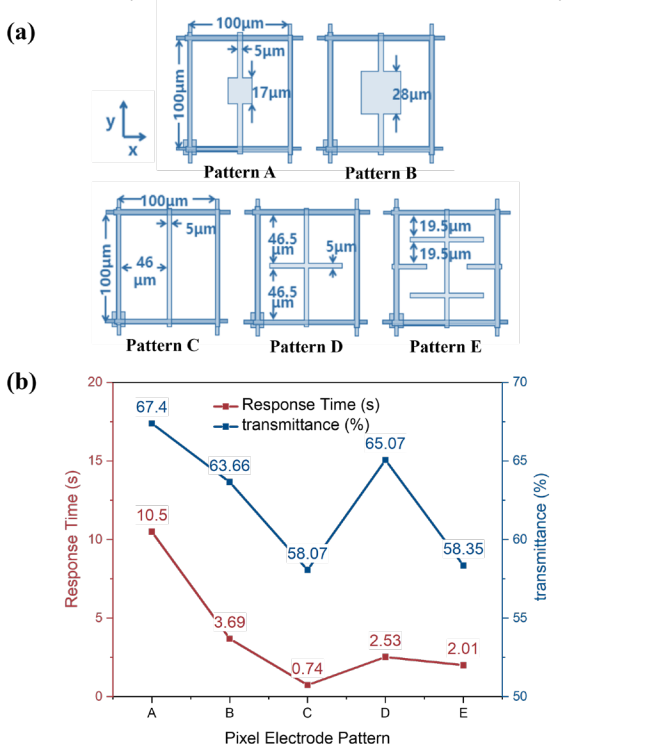

Fig 7. (a) Different pixel electrode designs (b) The transmittance and response time (white state to transparent state) of pattern A-E.

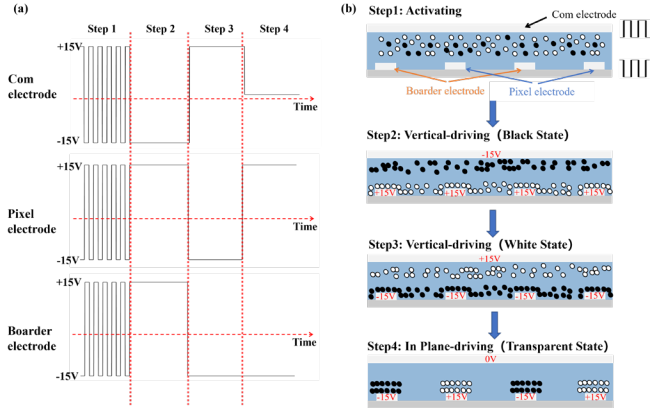

Fig 8. Waveform and driving diagram of 3D-driving EPD.

5. Conclusion

People are continuously exploring the integration of multifunctional electronic papers, striving to fully exploit the application potential of electronic paper. The three types of multifunctional electronic papers mentioned in this article effectively combine EPD with photoluminescence, electroluminescence, and 3D driving technology, respectively, achieving functions beyond reflective display, such as anti-counterfeiting, self-luminescence, and emissive-reflective switching. In the future, we will continue to explore more implementation methods of EPD+, allowing EPD technology to provide technological convenience to humans in a wider range of application scenarios.

6. Acknowledgement

This work was supported by MOST (2022YFA1203003).

7. Reference

[1] B. Comiskey, et al. *Nature,* 394**,** 253-255 (1998).
[2] B.-R. Yang. *E-paper Displays*[M]: John Wiley & Sons, 2022.
[3] B. R. Yang, et al. *Journal of the Society for Information Display,* 29**,** 38-46 (2021).
[4] M. Wang, et al. *SID Symposium Digest of Technical Papers,* 45**,** 857-860 (2014).
[5] Y. Zhang, et al. *Chemical Engineering Journal,* 497**,** 154666 (2024).
[6] R. Liang, et al. *The Spectrum,* 16 (2003).
[7] H. Lu, et al. *Advanced Fiber Materials***,** 1-13 (2024).
[8] Z. Qiu, et al. *Journal of Materials Chemistry C,* 11**,** 13244-13255 (2023).
[9] S. Zhu, et al. *Advanced Materials Technologies***,** 2400111 (2024).
[10] G. Liu, et al. *Light: Science & Applications,* 13**,** 198 (2024).
[11] J. Shi, et al. *Advanced Functional Materials***,** 2410139 (2024).
[12] G. Liu, et al. *Chemical Engineering Journal,* 470**,** 144133 (2023).
[13] J. Hong, et al. *Chemical Engineering Journal,* 439**,** 135726 (2022).
[14] X. Meng, et al. *ACS Applied Materials & Interfaces,* 5**,** 3638-3642 (2013).
[15] X. Zhu, et al. *Journal of Display Technology,* 1**,** 15 (2005).
[16] I. French, et al. *SID Symposium Digest of Technical Papers,* 54**,** 669-672 (2023).
[17] Q. Fan, et al. *Optics Letters,* 49**,** 2317-2320 (2024).
[18] S. Zhu, et al. *ACS Applied Materials & Interfaces,* (2024).
[19] M. Pietsch, et al. *Journal of Materials Chemistry C,* 7**,** 7121-7127 (2019).
[20] R. Huang, et al. *Chemical Engineering Journal,* 459**,** 141664 (2023).
[21] J.-T. Wu, et al. *ACS applied materials & interfaces,* 11**,** 14902-14908 (2019).
[22] Y. Zhang, et al. *Small***,** 2301886 (2023).
[23] B.-R. Yang, et al. U.S. Patent 8,681,191[P]. 2014-3-25.
[24] Y. Liu, et al. *Optics Express,* 31**,** 40102-40112 (2023).